UBR5 knockdown in human myotubes *in-vitro* and mouse skeletal muscle tissue *in-vivo* determines its pertinent role in anabolism and hypertrophy

Daniel C. Turner[1,2,3]*, David C. Hughes[4]*, Leslie M. Baehr[4], Robert A. Seaborne[3,5], Mark Viggars[3], Jonathan C. Jarvis[3], Piotr P. Gorski[1,2], Claire E. Stewart[3], Daniel J. Owens[3], Sue C. Bodine[4#] and Adam P. Sharples[1,2,3#]

[1]*Institute for Physical Performance, Norwegian School of Sport Sciences (NiH), Oslo, Norway*

[2]*Inst. for Science & Technology in Medicine (ISTM), School of Pharmacy and Bioengineering, Keele University, Staffordshire, UK*

[3]*Stem Cells, Ageing and Molecular Physiology Unit (SCAMP), Research Institute for Sport & Exercise Sciences (RISES), Liverpool John Moores University, Liverpool, UK*

[4]*Department of Internal Medicine, Division of Endocrinology and Metabolism, Carver College of Medicine, University of Iowa, Iowa City, IA, USA*

[5]*Centre for Genomics and Child Health, Blizard Institute, Barts and the London School of Medicine and Dentistry, Queen Mary University of London, UK*

* Joint Primary Authors. These authors contributed equally to this work.

Joint corresponding authors

Corresponding Authors Details:

Sue C. Bodine & Adam P. Sharples

Email: sue-bodine@uiowa.edu & a.p.sharples@googlemail.com

Abstract

UBR5 is an E3-ubiquitin-ligase positively associated with anabolism, hypertrophy and recovery from atrophy in skeletal muscle. The precise mechanisms underpinning UBR5's role in the regulation of skeletal muscle mass remain unknown. The present study aimed to investigate the mechanism of action of UBR5 by silencing the UBR5 gene *in-vitro* and *in-vivo*. The siRNA-induced reduction (-77%) in UBR5 gene expression in human myotubes was prevented by mechanical loading, suggesting that UBR5 gene expression was activated downstream of mechano-transduction signalling. MEK/ERK/p90S6K-signalling is an established mechano-sensitive-pathway involved in muscle anabolism/hypertrophy and importantly, has been shown to regulate UBR5 during growth of cancer cells. Therefore, we electroporated a UBR5 RNAi plasmid into mouse Tibialis Anterior muscle *in-vivo* to investigate the impact of reduced UBR5 on MEK/ERK/p90RSK-signalling. Electroporation resulted in a 55%/60% reduction in UBR5 mRNA/protein. Seven days post electroporation, while overall muscle mass was not significantly reduced, mean fibre CSA of GFP-positive fibres was reduced (-9.5%) and the number of large fibres were lower versus the control. Importantly, UBR5-RNAi significantly reduced total RNA, muscle protein synthesis (puromycin incorporation) and ERK1/2-phosphorylation. However, p90RSK-phosphorylation significantly increased, suggesting a potential compensatory mechanism following a reduction in UBR5. Finally, these acute changes evident after 7 days of UBR5 knockdown were exacerbated after 30 days, culminating in significant reductions in muscle mass (-4.6%) and fibre CSA (-18.5%). The present study supports the notion that UBR5 plays an important role in muscle anabolism/hypertrophy, and that a reduction in UBR5 is associated with alterations in ERK1/2 and p90RSK that culminates in atrophy.

Running title: UBR5 knockdown reveals its important role in anabolism and hypertrophy

Keywords UBR5, siRNA, RNAi, Myotubes, Skeletal Muscle, Mechanical Loading, Hypertrophy, Electroporation, MAPK, MEK, MSK, ERK, p90RSK

Introduction

The regulation of skeletal muscle (SkM) mass is orchestrated by the activity of key signalling pathways that control protein breakdown and synthesis within myofibres. The breakdown or atrophy of SkM mass is mediated predominantly by the ubiquitin-proteasome system (Cao *et al.*, 2005; Bodine & Baehr, 2014), composed of three key enzymes that activate and conjugate (E1 & E2 enzymes) small ubiquitin molecules to target protein substrates (E3 ligases) for recognition and subsequent degradation in the prevalent 26S proteasome system. The best characterised E3 ubiquitin ligases associated with SkM atrophy are the muscle specific RING finger protein 1 (MuRF1 or Trim63) and the F-box containing ubiquitin protein ligase atrogin-1 (Atrogin-1; Gomes *et al.*, 2001), otherwise known as muscle atrophy F-box (MAFbx; Bodine *et al.*, 2001*a*).

Interestingly, recent work by our group identified that a HECT domain E3 ligase named ubiquitin protein ligase E3 component n-recognin 5 (UBR5, also termed EDD1) was significantly altered at the DNA methylation and gene expression level following resistance exercise (RE) in human SkM (Seaborne *et al.*, 2018*b*, 2018*a*). UBR5 DNA methylation decreased (hypomethylation) and mRNA expression increased after 7 weeks of training-induced SkM hypertrophy, with even greater changes reported following a later 7 weeks of retraining (Seaborne *et al.*, 2018*b*, 2018*a*). The pattern observed in DNA methylation and gene expression, which correlated significantly with changes in lean mass, suggested a role for UBR5 during muscle hypertrophy in contrast to E3 ligases, MuRF1 and MAFbx that are associated with atrophy. Additional work by our group has provided further support for this hypothesis whereby UBR5 expression significantly increased after acute loading in bioengineered SkM, in response to synergistic ablation/functional overload (FO), and after programmed resistance training in rodent muscle with no change in MuRF1 and MAFbx expression (Seaborne *et al.*, 2019). UBR5 also increased during recovery from hindlimb unloading (HU) and disuse atrophy, with no increase in MuRF1 and MAFbx (Seaborne *et al.*, 2019). Furthermore, increased gene expression of UBR5 in these models resulted in greater abundance of UBR5 protein content following FO-induced hypertrophy of the mouse plantaris muscle *in-vivo*, and over the time-course of regeneration in primary human muscle cells *in-vitro* (Seaborne *et al.*, 2019). A recent study also supported the role of UBR5 as being essential for muscle growth through RNAi screening in *Drosophila* larvae, where UBR5 inhibition led to smaller sized larvae (Hunt *et al.*, 2019). Finally, unpublished data from our lab in bioengineered mouse SkM also demonstrated that UBR5 was the most significantly upregulated transcript after loading, amongst a selection of genes that are known to be regulated across the human transcriptome and methylome after acute RE (Seaborne *et al.*,

2018*b*; Turner *et al.*, 2019*b*). Collectively, these data support the notion that UBR5 is involved in load-induced anabolism and hypertrophy, in contrast with the well-known MuRF1 and MAFbx E3 ligases that are associated with muscle atrophy.

The best characterised signalling pathway involved in protein synthesis and hypertrophy of SkM is the mammalian target of rapamycin complex 1 (mTORC1) pathway (Baar *et al.*, 2000; Bodine *et al.*, 2001; Goodman *et al.*, 2011). Work by the Esser laboratory reported PI3K/Akt-independent activation of mTOR via mitogen-activated protein kinase (MEK)/extracellular signal-regulated kinase (ERK) signalling which was critical for overload-induced hypertrophy (Miyazaki *et al.*, 2011). Moreover, earlier work demonstrated increased ERK1/2 phosphorylation after acute resistance exercise (RE) in humans (Drummond *et al.*, 2009) and after mechanical loading in C_2C_{12} myotubes (Hornberger *et al.*, 2005). Further, downstream of ERK1/2, phosphorylation of the ribosomal S6 kinase, p90RSK is increased with acute endurance and resistance exercise in rodent and human SkM (Yu *et al.*, 2001; Williamson *et al.*, 2003; Moore *et al.*, 2011). Interestingly, previous work suggests that UBR5 is regulated via ERK/p90RSK signalling in non-muscle cells (Cho *et al.*, 2017). Indeed, UBR5 has been shown to be a target substrate for ERK2 in the COS-1 kidney fibroblast cell line after treatment with epidermal growth factor (EGF), an established ligand that initiates downstream ERK signalling when bound to its receptor (EGFR) (Eblen *et al.*, 2003). Others have also shown that p90RSK, phosphorylates UBR5 in HeLa cancer cells at various sites, and may therefore be involved in growth of cancer cells (Cho *et al.*, 2017). However, there are no studies to date investigating the interaction between UBR5 and MEK/ERK/p90RSK signalling in SkM. Manipulation of UBR5 is therefore required to elucidate its mechanistic role in regulating muscle mass.

In the present study, we first aimed to silence UBR5 in human myotubes during mechanical loading to confirm its regulatory role in response to loading. We demonstrate that while siRNA-induced silencing of UBR5 reduced gene expression by ~77%, this reduction in expression was completely prevented by the addition of mechanical loading, which suggests that UBR5 gene expression is activated downstream of mechano-transduction signalling. Therefore, we used a miR-based RNAi for UBR5 using pcDNA TM 6.2-GW/EmGFP-miR electroporated into murine tibialis anterior (TA) muscle, to investigate the impact of reduced UBR5 on MEK/ERK/p90RSK signalling *in-vivo*. UBR5 RNAi reduced UBR5 gene expression by 55% and protein levels by 60% in the TA of mice after 7 days electroporation. UBR5 silencing also led to a reduction in the CSA of transfected fibres, the frequency of larger fibres (≥3400 μm^2), total RNA content, protein synthesis and ERK1/2 activity.

Surprisingly however, p90RSK activity increased, which may reflect a compensatory mechanism in response to reduced UBR5. Finally, the changes at 7 days also culminated in significant reductions in muscle mass and fibre CSA after prolonged transfection (30 days). Overall, we demonstrate that UBR5 is an important positive regulator of muscle mass via altered ERK1/2 and p90RSK signalling.

Methods

Skeletal Muscle Tissue and Ethical Approval

Prior to collection of human muscle tissue, participants gave written informed consent. Ethical approval was granted by the NHS West Midlands Black Country, UK, Research Ethics Committee (NREC approval no. 16/WM/0103). Muscle tissue was handled and stored in accordance with Human Tissue Act (2004) regulations. For *in-vitro* myotube experiments, human skeletal muscle biopsies were obtained from the vastus lateralis muscle of three young healthy males (23 ± 3.2 yrs, 75.4 ± 3.7 kg, 180.7 ± 2.1 cm, BMI 23.1 ± 1.5 kg/m^2) using a needle biopsy instrument (CR Bard, Crawley, UK) as described fully elsewhere (Turner *et al.*, 2019*a*). For *in-vivo* muscle tissue experiments, C57Bl/6 male mice between twelve and sixteen weeks-old (*n* = 10) were obtained from Charles River Laboratories for electroporation experiments. All animal procedures were approved by the Institutional Animal Care and Use Committee at the University of Iowa. During tissue collection, animals were anaesthetized with 2–3% inhaled isoflurane. On completion of tissue removal, mice were euthanised by exsanguination.

Isolation and Culture of Human Skeletal Muscle Derived Cells (HMDCs)

Following human biopsy procedures, muscle tissue was placed in sterile microfuge tubes (Ambion®, Thermo Fisher Scientific Denmark) containing 1.5 ml of chilled (4˚C) transfer media composed of Ham's F-10 medium including 1 mM L-glutamine (LG; Thermo Fisher Scientific, Denmark), 0.1% heat inactivated fetal bovine serum (hiFBS; Gibco™, South America Origin, Fisher Scientific, UK), 0.1% heat inactivated new born calf serum (hiNBCS; Gibco, New Zealand Origin, Fisher Scientific, UK), 100 U/ml penicillin (Lonza, UK), 100 µg/ml streptomycin (Lonza, UK), 2.5 µg/ml amphotericin B (Sigma-Aldrich, UK) and transported on ice to a class II biological safety cabinet (Kojair Biowizard Silverline, Finland) to undergo subsequent cell isolations as described in previous work by our group (Crown *et al.*, 2000; Owens *et al.*, 2015; Turner *et al.*, 2019*a*). Briefly, muscle tissue was minced in 5 ml trypsin (0.05%)/EDTA (0.02%) solution using 2 × sterile scalpels (No. 11, Swann-Morton, UK). The contents were transferred to a sterile specimen pot to enable magnet stirring at 37˚C for 10 mins. This process was repeated, and then homogenised tissue was placed in a sterile 15 ml tube (Falcon®, Fisher

Scientific, UK) containing 2 ml heat inactivated horse serum (hiHS; Gibco™, New Zealand Origin, Fisher Scientific, UK) to neutralise the trypsin. The tube was centrifuged (340 × g for 5 min at 24˚C) and the supernatant was seeded on to 2 separate pre-gelatinised (0.2% in dH_2O; Type A, Sigma-Aldrich, UK) T25 flasks (Nunc™, Thermo Fisher Scientific, Denmark) containing 7.5 ml of growth medium (GM, composed of Ham's F-10 medium that included 1 mM LG, 10% hiFBS, 10% hiNBCS, 4 mM LG, 100 U/ml penicillin, 100 µg/ml streptomycin and 2.5 µg/ml amphotericin B). Both flasks were then incubated (HERAcell 150i CO_2 humidified incubator, Thermo Fisher Scientific, Denmark) at 37˚C and 5% CO_2 until ~80% confluency was attained. Cells were then transferred to T75 flasks and passaged (P7-9) until sufficient cell quantities were acquired for experimentation.

Transfection of UBR5 siRNA into Human Myotubes

After serial passaging, HMDCs (passage 7-9) were seeded onto plastic 6-well fibronectin-coated (10 µg/ml in PBS, Sigma-Aldrich, UK) culture plates (described below) at a density of 9×10^4 cells/ml in 2 ml GM. Once ~80% confluency was attained (Figure 1A), medium was switched to 2 ml differentiation media (DM; same media components as GM with the exception of lower 2% hiFBS) for the remaining 10 days. Each well received an additional 1 ml of DM as a top up at 72 hrs (Figure 1B) and 7 days (Figure 1C). At day 10 (Figure 1D), the resulting myotubes received either 750 µl DM alone or 750 µl DM containing 9 µl HiPerFectTransfection™ (Qiagen, UK) and 20 nmol Flexitube GeneSolutions™ (siUBR5, Qiagen, UK). The Flexitube GeneSolutions includes 4 × siRNA's that target multiple regions of the 10900 bp UBR5/EDD1 human gene (Figure 2) and evoked a 77 ± 1.28% (mean ± SEM) reduction in UBR5 gene expression after 3 hours when using a 20 nmol concentration. Also, using a scramble siRNA (Qiagen, AllStars Negative Control siRNA™ including HiPerFectTransfection reagent) we confirm that we saw no significant reduction in UBR5 at this 3h time point. Please note that we first established the recommended 10 nmol siRNA concentration did not reduce UBR5 gene expression substantially (reduction of only 25.72 ± 4.72%) in human myotubes and that higher concentrations were therefore required during loading experiments.

Mechanical Loading of Myotubes

HMDCs were first differentiated on fibronectin-coated (10 µg/ml in PBS, Sigma-Aldrich, UK) flexible-bottomed culture plates (25 mm BioFlex®, Dunn Labortecknik, Germany) for 10 days as described above (see Figure 1). Resultant myotubes were dosed with either 20 nmol UBR5 siRNA or DM alone, immediately after which, loading experiments commenced. Myotubes were subjected to equibiaxial tension using the Flexcell® FX-5000™ Tension system (Dunn Labortecknik, Germany) and a low

frequency (0.15 Hz with sine wave) intermittent loading regime was applied (see Figure 1E and F). The loading regime consisted of 4 sets of 10 repetitions with 90 s rest between sets, representing 1 loading session. This was repeated 5 times with each loading session interspersed with a 3.5 min rest, totalling a regime of 60 mins. Non-loaded control myotubes were also assembled in the Flexcell® base plate, however, the vacuum entry was sealed to avoid any unwanted loading. Following cessation of mechanical loading, both loaded and non-loaded myotubes were lysed for RNA at '0 hrs' (30 mins) and 3 hrs incubation. Due to the low number of human cells available for these experiments, protein extraction for e.g. ERK/P90RSK signalling analysis was not possible.

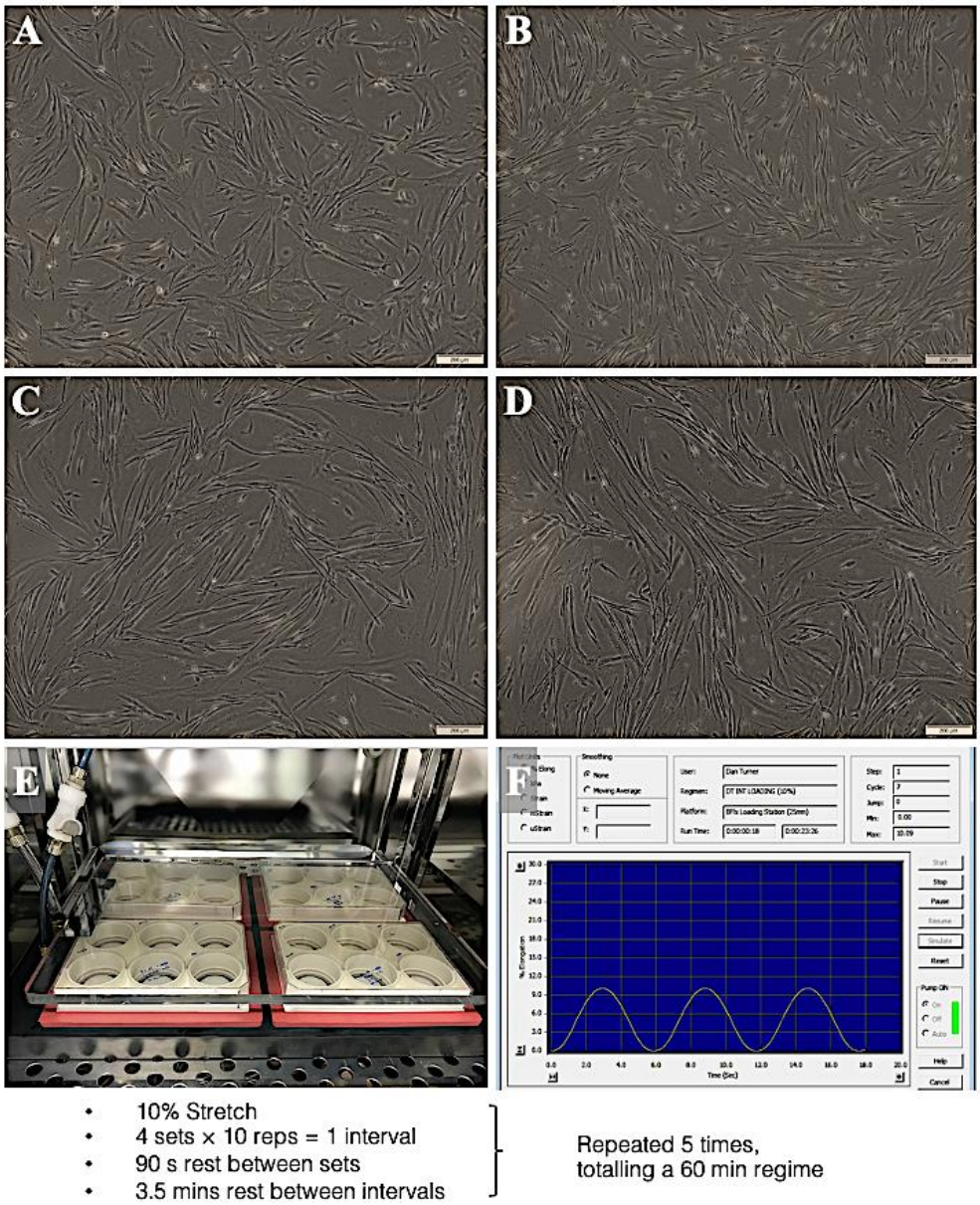

Figure 1. Differentiation and mechanical loading of human myotubes. Cultured HMDCs at **(A)** 0 hrs, **(B)** 72 hrs, **(C)** 7 days and **(D)** 10 days in DM (10× magnification, Olympus, CKX31) **(E)** HMDCs cultured and mechanically loaded on BioFlex® well plates within a humidified incubator at 37˚C/5%. **(F)** Example of the sine wave profile during the mechanical loading regime.

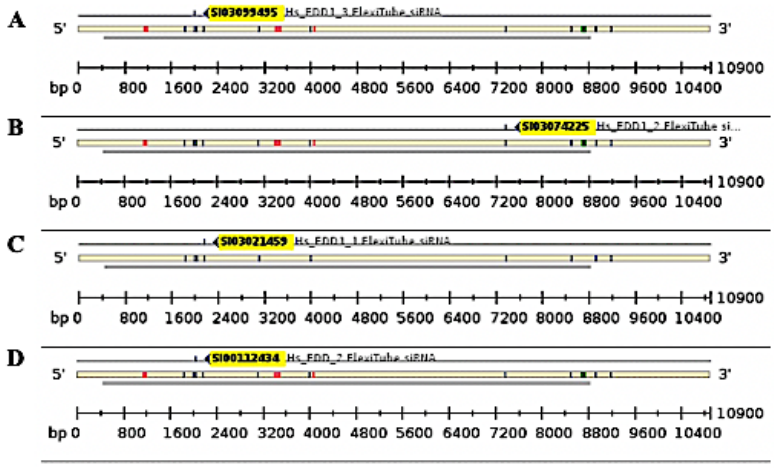

E

Product Name	Target Sequence
Hs_EDD1_3	CTGGTATTTCTTCAATGCCGA
Hs_EDD1_2	CCAAATCTAGAGTGTATCCAA
Hs_EDD1_1	TTCAACTTAGATCTCCTGAAA
Hs_EDD_2	CAGGTATGCTTGAGAAATAAT

Figure 2. Graphical representation of the 4 × siUBR5 sequence locations (NM_015902, 10900 bp length) of the EDD1/UBR5 human gene. **(A)** Hs_EDD1_3. **(B)** Hs_EDD1_2.03 **(C)** Hs_EDD1_1. **(D)** Hs_EDD_2. **(E)** UBR5/EDD1 siRNA sequences.

Plasmid Design and Electroporation

An RNAi system which was designed and purchased from Invitrogen (Thermo Fisher Scientific, *USA*) was implemented. Specifically, the negative control/empty vector (EV) RNAi plasmid was described previously (Ebert *et al.*, 2012; Seaborne *et al.*, 2019) and encodes emerald green fluorescent protein (EmGFP) and a non-targeting pre-miRNA under bicistronic control of the CMV promoter in the pcDNA6.2GW/EmGFP-miR plasmid (Invitrogen). The UBR5 RNAi plasmid also encodes EmGFP plus an artificial pre-miRNA targeting mouse UBR5 under bicistronic control of the CMV promoter. It was generated by ligating the Mmi571982 oligonucleotide duplex (Invitrogen) into the pcDNA6.2GW/EmGFP-miR plasmid. The UBR5 RNAi plasmid is designed to target the nucleotide sequence in the HECT domain between amino acids positions 2695-2754 (highlighted in yellow on Figure 3A). The electroporation technique was performed as previously described (Seaborne *et al.*, 2019). Briefly, after a 2hr pre-treatment with 0.4 units/ul of hyaluronidase, 20 µg plasmid DNA was injected into the tibialis anterior (TA) muscle and the hind limbs were placed between two-paddle electrodes and subjected to 10 pulses (20 msec) of 175 V/cm using an ECM-830 electroporator (BTX Harvard Apparatus). Mice were injected with the UBR5 RNAi plasmid and an empty vector (EV) control into the contralateral muscle. TA muscles were harvested after 7 and 30 days.

Mouse Skeletal Muscle Tissue Collection

Following completion of the appropriate time period, mice were anesthetized with isoflurane, and the TA muscles were excised, weighed, frozen in liquid nitrogen, and stored at −80°C for later analyses. Muscles were collected for histology (n = 5) and RNA/Protein isolation (n = 5) and processed as described below. On completion of tissue removal, mice were euthanized by exsanguination.

Immunohistochemistry and Histology

Cultured HMDCs were washed 3 × TBS (1×; Sigma-Aldrich, UK) and fixed in ice-cold methanol:acetone:TBS (25:25:50 for 15 mins) then in methanol:acetone (50:50) for a further 15 mins. Following fixation, HMDCs were permeabilised in 0.2% Triton X-100 (Sigma-Aldrich, UK) and blocked in 5% goat serum (Sigma-Aldrich, UK) in TBS for 90 mins. Cells were washed 3 × in TBS and incubated overnight (4˚C) in 300 µl of anti-desmin (ab15200, Abcam, UK) primary antibody made up in TBS, 2% goat serum and 0.2% Triton X-100 at concentrations of 1:50. After overnight incubation, the primary antibody was removed and HMDCs were washed 3 × in TBS. Cells were incubated at RT for 3 hrs in 300 µl secondary antibody solution containing anti-rabbit TRITC (T6778, Sigma-Aldrich, UK) at a concentration of 1:75 in 1× TBS, 2% goat serum and 0.2% Triton X-100 to counterstain myoblasts. After a further 3 × TBS washes, 300 µl of DAPI (D1306, Thermo Fisher Scientific, Denmark) was added to the cells at a concentration of 300 nM for 30 mins to counterstain myonuclei. Immunostained HMDCs were visualised and imaged using confocal microscopy (Olympus IX83, Japan) with TRITC (Excitation: 557 nm, Emission: 576 nm) and DAPI (Excitation: 358 nm, Emission: 461 nm) filter cubes. Immuno-images were imported to Fiji/ImageJ (version 2.0.0) software to determine myogenicity via counting the total number of myoblasts overlapping nuclei divided by the total number of nuclei present (myogenic proportions 72 ± 2.4%). Harvested mouse TA muscles were immediately weighed and fixed in 4% (w/v) paraformaldehyde for 16 h at 4˚C and then placed in 30% sucrose for overnight incubation. The TA muscles were then embedded in Tissue Freezing Medium (Triangle Biomedical Sciences), and a Thermo HM525 cryostat was used to prepare 10 µm sections from the muscle mid-belly. All sections were examined and photographed using a Nikon Eclipse Ti automated inverted microscope equipped with NIS-Elements BR digital imaging software.

Laminin Stain

TA muscle sections were permeabilized in PBS with 1% triton for 10 minutes at room temperature. After washing with PBS, sections were blocked with 5% goat serum for 15 minutes at room temperature. Sections were incubated with Anti-Laminin (1:500, Sigma Aldrich, Cat no. L9393) in 5% goat serum for 2 hours at room temperature, followed by two 5-minute washes with PBS. Goat-anti-rabbit AlexaFluor® 555 secondary (1:333) in 5% goat serum was then added for 1 hour at room temperature. Slides were cover slipped using ProLong Gold Antifade reagent (Life Technologies). Image analysis was performed using Myovision software (Wen *et al.*, 2018). Skeletal muscle fibre size was analyzed by measuring ≥ 250 transfected muscle fibres per muscle, per animal (10x

magnification). Transfected muscle fibres were identified as GFP-positive as shown in Figure 5B (7 days) and 7B (30 days).

RNA Extraction, Primer Design and Polymerase Chain Reaction (PCR) (Human myotubes)

After incubation, existing media was removed and myotubes were washed 2 × in PBS before lysing cells with 300 µl TRIzol (Invitrogen™, Thermo Fisher Scientific, Denmark) for subsequent RNA extraction. RNA concentrations (76.64 ± 57.94 ng/µl, mean ± SD) and purities (A_{260}/A_{280} ratio, 1.91 ± 0.22, mean ± SD) were quantified using a spectrophotometer (NanoDrop™ 2000, Thermo Fisher Scientific, Denmark). A one-step PCR kit (QuantiFast™ SYBR® Green, Qiagen, UK) was used to assess gene expression. Firstly, samples were diluted in nuclease-free H_2O to ensure a concentration of 35 ng RNA in 10 µl reactions, made up of: 4.75 µl (7.37 ng/µl) RNA sample and 5.25 µl of master mix (MM) composed of 5 µl SYBR green mix, 0.1 µl of reverse transcriptase (RT) mix and 0.075 µl of both forward and reverse primers (both at 100 µM). Primers were designed using both Clustal Omega (https://www.ebi.ac.uk/Tools/msa/clustalo/) and Primer-BLAST (NCBI, https://www.ncbi.nlm.nih.gov/tools/primer-blast/) and were purchased from Sigma-Aldrich. All primer sequence information is described in Table 1. PCR reactions were transferred to a qRT-PCR machine (Rotorgene 3000Q, Qiagen, UK) with supporting software (Hercules, CA, USA) to undergo amplification as follows: 10 min hold at 50˚C (reverse transcription/cDNA synthesis), 95˚C for 5 min (transcriptase inactivation and initial denaturation step) and PCR Steps of 40 cycles; 95˚C for 10 s (denaturation), 60˚C for 30 s (annealing and extension). Upon completion, melt curve analyses was carried out to identify non-specific amplification or primer-dimer issues for the reference genes and UBR5. These analyses demonstrated a single melt peak for all genes. Gene expression was then quantified using the DDCT ($2^{-\Delta\Delta}$CT) equation (Schmittgen & Livak, 2008) against the mean of 2 reference genes (B2M and RPL13a, 15.33 ± 0.7 with low variation across all conditions of 4.56%) and the mean C_T value derived from the non-treated DM group for each time point (0/3 hrs) and condition (non-loaded/loaded). The PCR efficiencies were similar for the reference genes, RPL13a (97.4 ± 7.75%, with 7.96% variation) and B2M (92.08 ± 3.18%, with 3.46% variation), and the gene of interest, UBR5 (90.93 ± 4.94%, with 5.43% variation).

Table 1. Primer sequence information for genes analysed in human myotubes (h) and mouse SkM (m).

Target Gene	Primer Sequence (5'-3')	Product Length (bp)
UBR5 (h)	F: AGGCAACACCTTAGGAAGC	81
	R: GCTCCAGCTGATGACCTAC	
RPL13a (h)	F: GGCTAAACAGGTACTGCTGGG	104
	R: GGAAAGCCAGGTACTTCAACTT	
B2M (h)	F: CCGTGTGAACCATGTGACT	91
	R: TGCGGCATCTTCAAACCT	
UBR5 (m)	F: GTCTGCTGGAGCTCGTGATT	106
	R: TGCTGGAATAACTGGCTGGG	

RNA isolation and gene expression (Mouse Muscle tissue)

Prior to RNA isolation, aliquots of frozen muscle powder were weighed in order to calculate RNA per milligram of wet muscle tissue. cDNA was synthesized using a reverse transcription kit (iScript cDNA synthesis kit; Bio-Rad, Hercules, CA) from 1 µg of total RNA. PCR reactions (10 µL) were set up as: 2 µL of cDNA, 0.5 µL (10 µM stock) forward and reverse primer, 5 µL of Power SYBR Green master mix (Thermo Fisher Scientific, Waltham, MA) and 2 µL of RNA/DNA free water. Gene expression analysis was performed by quantitative PCR on a Quantstudio 6 Flex Real-time PCR System (Applied Biosystems, Foster City, CA) using the mouse primers shown in Table 1. PCR cycling comprised: hold at 50°C for 5 min, 10 min hold at 95°C, before 40 PCR cycles of 95°C for 15 s followed by 60°C for 1 min (combined annealing and extension). Melt curve analysis at the end of the PCR cycling protocol yielded a single peak. Because of reference gene instability, gene expression was normalized to tissue weight and subsequently reported as the fold change relative to empty vector (EV) muscles, as described previously (Heinemeier *et al.*, 2009). This type of analysis has previously been used extensively by our group (Baehr *et al.*, 2016, 2017; Hughes *et al.*, 2018) and demonstrated a significant 55% reduction in UBR5 gene expression after 7 days UBR5 RNAi (Figure 3B).

Muscle Protein Synthesis (MPS)

Changes in MPS were assessed in TA muscles transfected for 7 days by measuring the incorporation of exogenous puromycin into nascent peptides as described previously (Goodman *et al.*, 2011*b*; West *et al.*, 2016). Puromycin (EMD Millipore, Billerica, MA, USA; cat. no. 540222) was dissolved in sterile saline and delivered (0.02 µmol g^{-1} body weight by I.P. injection) 30 min prior to muscle collection.

Immunoblotting

Frozen TA muscles were homogenized in sucrose lysis buffer (50 mM Tris pH 7.5, 250 mM sucrose, 1 mM EDTA, 1 mM EGTA, 1% Triton X 100, 50 mM NaF). The supernatant was collected following centrifugation at 8,000 *g* for 10 minutes and protein concentrations were determined using the 660-protein assay (Thermo Fisher Scientific, Waltham, MA). Twelve micrograms of protein were subjected to SDS-PAGE on 4-20% Criterion TGX stain-free gels (Bio-Rad, Hercules, CA) and transferred to polyvinylidene diflouride membranes (PVDF, Millipore, Burlington, MA). Membranes were blocked in 3% nonfat milk in Tris-buffered saline with 0.1% Tween-20 added for one hour and then probed with primary antibody (concentrations detailed below) overnight at 4°C. Membranes were washed and incubated with HRP-conjugated secondary antibodies at 1:10,000 for one hour at room temperature. Immobilon Western Chemiluminescent HRP substrate was then applied to the membranes prior to image acquisition. Image acquisition and band quantification were performed using the Azure C400 System (Azure Biosystems, Dublin, CA, USA) and Image Lab, version 6.0.1 (Bio-Rad), respectively. Total protein loading of the membranes captured from images using stain-free gel technology was used as the normalization control for all blots. The following primary antibodies were used all used at a concentration of 1:1000: Cell Signaling Technologies (Danvers, MA, USA) – phospho-ERK $^{Thr202/Tyr204}$ (cat. 4370), phospho-p90RSK ^{Ser380} (cat. 11989), phospho-MSK1 ^{Thr581} (cat. 9595), phospho-MEK1/2 $^{Ser217/221}$ (cat. 9154), UBR5 (cat. 65344), GFP (cat. #2956) and EMD Millipore – puromycin (cat. MABE343). Knockdown of UBR5 protein was confirmed previously with a reduction of 60% (Seaborne *et al.*, 2019; Figure 3C) and MAPK signaling antibodies in the present study were processed on the same samples as this UBR5 protein data.

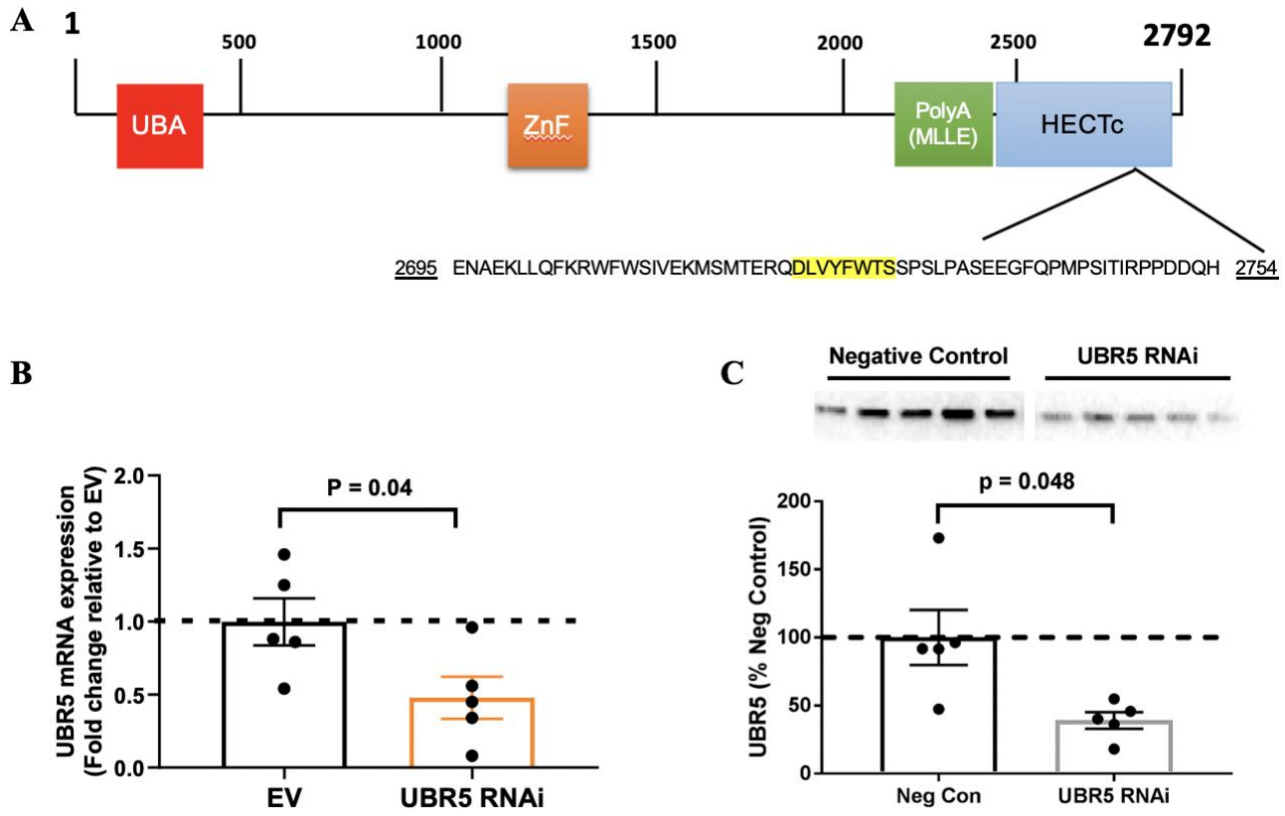

Figure 3. Graphical schematic of UBR5 protein structure and confirmation of UBR5 knockdown in tibialis anterior (TA) skeletal muscle after 7 days electroporation. (A) Putative domain structure of UBR5 protein consists of ubiquitin-associated (**UBA**) domain-like superfamily, Putative zinc finger in N-recognin (**ZnF**), Poly-adenylate binding protein (**PolyA**), MLLE protein/protein interaction domain and a HECT domain. The UBR5 RNAi plasmid is designed to target the nucleotide sequence in the HECT domain between amino acids position 2695-2754 (highlighted in yellow). (**B**) After initial screening, we identified a possible RNAi candidate (Mmi571982; Invitrogen) for UBR5 knockdown. TA skeletal muscles were transfected for 7 days and we observed ~55% reduction in UBR5 mRNA expression relative to empty vector (EV) transfected muscles. Thus, we confirmed that the RNAi plasmid significantly reduces UBR5 mRNA and protein levels (see reference Seaborne et al., 2019) in basal mouse skeletal muscle. (**C**) We have previously confirmed significant reductions in UBR5 protein levels in the same samples with this UBR5 RNAi plasmid (figure therefore taken from; R. A. Seaborne et al., *Journal of Physiology* (Wiley), 597.14 (2019) pp 3727–3749, with permissions, Copyright-2019 The Authors. *The Journal of Physiology*. Copyright-2019 The Physiological Society). Data presented as Mean ± SEM. (N = 5 per group). Statistical significance is depicted where present ($P \geq 0.05$).

Statistical Analysis

Paired student *t-tests* were first carried out to assess knockdown efficiency (%) in siUBR5 treated vs. DM non-treated cells at 0 and 3 hrs in loaded and non-loaded myotubes and then to determine the significance of UBR5 mRNA fold-change in loaded vs. non-loaded myotubes dosed with DM alone. Finally, paired *t-tests* were carried out when comparing empty control (EV) vs. UBR5 RNAi transfected mouse TA SkM. All statistical analysis was performed using GraphPad Software (Prism,

Version 7.0a, San Diego, CA). Data is presented as mean ± standard error of the mean (SEM). $P \leq 0.05$ represents statistical significance.

Results

Impact of mechanical loading on UBR5 gene expression in human myotubes

Given previous work by our group showing increased UBR5 mRNA expression after acute loading in C_2C_{12} bioengineered SkM (Seaborne *et al.*, 2019), chronic high-frequency electrical stimulation in rats (Schmoll *et al.*, 2018; Seaborne *et al.*, 2019) and acute/chronic RE in humans (Seaborne *et al.*, 2018*b*, 2018*a*, 2019), we wished to determine the impact of mechanical loading on UBR5 gene expression in human myotubes. Despite an increase in mean UBR5 gene expression at 3 hrs post-loading (1.58-fold ± 0.65), this change did not reach statistical significance ($P = 0.42$; see Figure 4A). This may be because cultured myotubes from one donor showed little change after loading whereas those from the other donors showed an increase. Although significance was not attained, on average, this was the same fold increase in UBR5 gene expression observed after loading in C_2C_{12} bioengineered SkM (1.58 fold) (Seaborne *et al.*, 2019) and similar to that observed in human tissue after acute RE (1.71 fold) (Seaborne *et al.*, 2018*b*, 2018*a*), thus warranting further investigation in human muscle cells.

siRNA induced reductions in UBR5 gene expression are prevented with mechanical loading

UBR5 gene expression following siRNA treatment in non-loaded (0 hrs and 3 hrs post dosing) and loaded (3 hrs post-dosing) human myotubes was determined. Following 3 hrs siRNA treatment the significant decrease in UBR5 gene expression evident in non-loaded cells (77% ± 1.28% $P < 0.001$; Figure 4B) was prevented by loading, demonstrated by a return to baseline levels of UBR5 expression (Figure 4B).

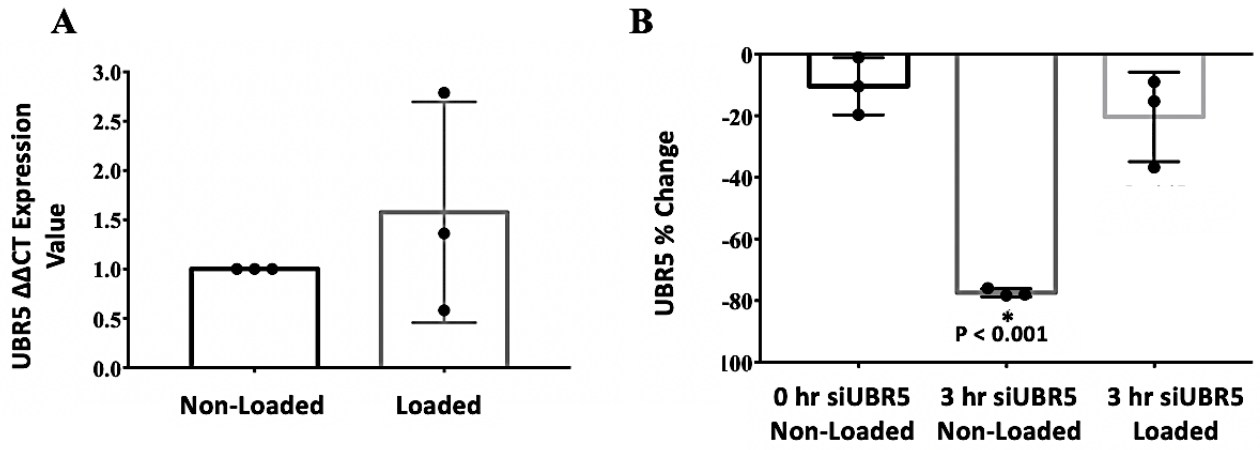

Figure 4. UBR5 gene silencing and mechanical loading in human myotubes. (A) UBR5 mRNA expression demonstrated a non-significant increase (1.58 ± 0.65, *P* = 0.42) in loaded versus non-loaded myotubes. **(B)** Silencing UBR5 reduced UBR5 mRNA expression (~77%) in human myotubes after 3 hours. Mechanical loading rescued UBR5 mRNA expression back towards baseline levels at 3 hrs post-loading. (*****) Depicts statistical significance ($P \leq 0.05$). Data is present as mean ± standard error of mean (SEM), *n* = 3 participants were used for all conditions, treatments and timepoints.

Fibre CSA, but not skeletal muscle mass was significantly reduced at 7 days post electroporation in mice

To examine the effect of reducing UBR5 expression *in-vivo*, mouse TA muscles were transfected with either UBR5 RNAi or an EV control. The TA mass (mg) did not significantly change at 7 days post electroporation in UBR5 RNAi vs. EV transfected TA muscle (Figure 5A). Interestingly, however, measurement of the CSA of GFP-positive fibres revealed that the mean fibre CSA of GFP-positive fibres was significantly reduced (-9.5 ± 3.2%) in RNAi transfected TA muscle (*P* = 0.048; Figure 5B & C) with fewer larger fibres (≥3400 μm^2) present versus the EV (Figure 5B & D).

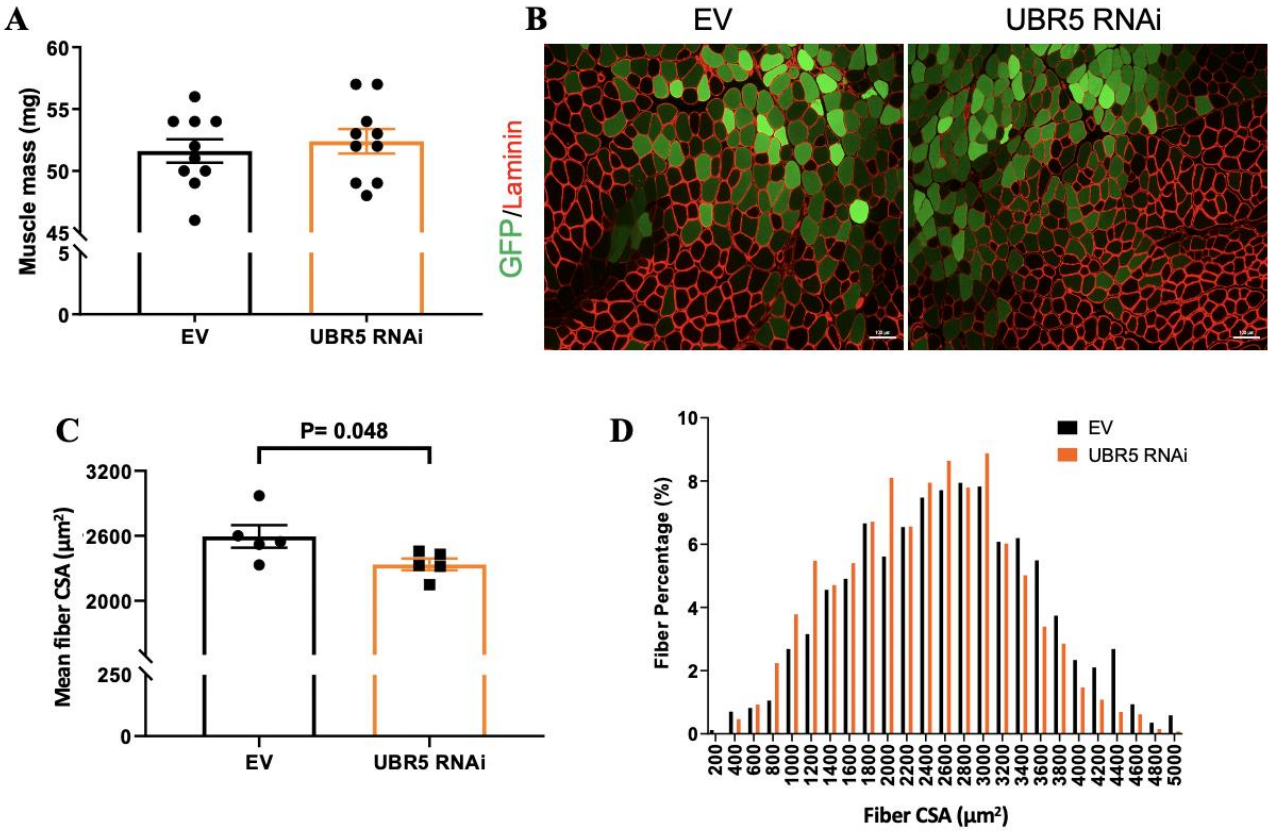

Figure 5. Muscle mass and fibre CSA in UBR5 RNAi transfected TA muscle after 7 days. (A) After 7 days, muscle mass was no different between empty vector control (EV) and UBR5 RNAi transfected TA muscles (*n* = 10 per group). (**B)** Representative images (10x magnification; scale bar = 100 µm) for GFP transfected fibre identification and CSA quantification through Laminin staining. **(C)** A significant reduction (*P* = 0.048) in mean transfected fibre CSA size was observed in the RNAi transfected vs. EV muscles *(n* = 5 per group). **(D)** Quantification of muscle CSA revealed increases in the percentage of small fibres (<1200 µm^2) and reductions in the percentage of large fibres (≥3400 µm^2) with RNAi transfected muscles verses EV group (**D**). Data presented as Mean ± SEM.

Total RNA concentrations, muscle protein synthesis and ERK1/2 signalling are reduced in UBR5 RNAi TA muscle after 7 days, however p90RSK phosphorylation is increased

Along with a reduction in fibre CSA at 7 days post UBR5 RNAi, a significant reduction in total RNA concentrations (*P* = 0.01, Figure 6A) and protein synthesis (17 ± 3.2% reduction, *P* = 0.05, Figures 6B & C) was evident. Wishing to determine potential regulators of this process, ERK1/2 (p44/42 MAPK) signaling was examined and found to be dampened (43 ± 2.3% reduction, *P* = 0.03, Figures 6D & F). Interestingly, the reduction in RNA, protein synthesis and ERK1/2 signalling coincided with a significant increase in phospho-p90RSK^{Ser380} (170% ± 39.8% increase, *P* = 0.04; Figure 6E & F) at this time point. We observed no differences in the phosphorylation of MSK-1^{Thr581} or MEK 1/2$^{Ser\ 217/221}$ between RNAi and EV transfected TA muscles after 7 days (Figure 6F).

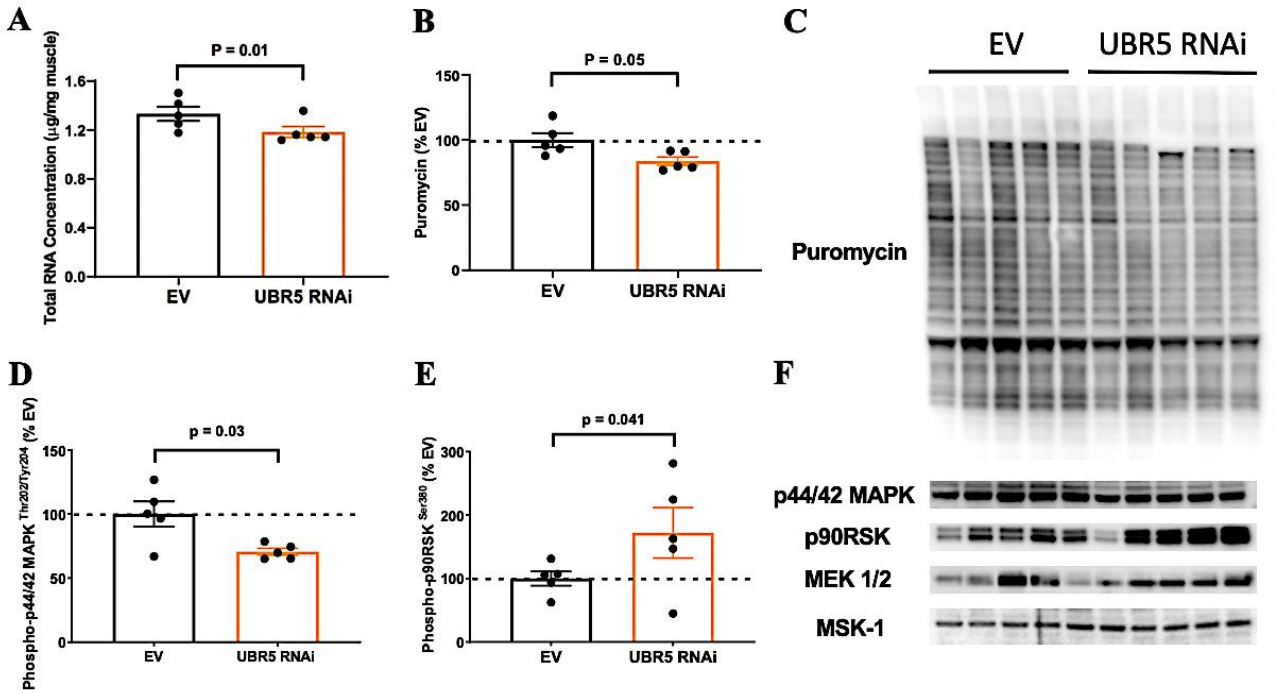

Figure 6. Alteration in total RNA, protein synthesis and MAPK/ERK/RSK signalling in UBR5 RNAi transfected TA muscle after 7 days. (A) Total RNA concentration (assessed as µg/mg of muscle) was significantly reduced (*P* = 0.01) in the UBR5 RNAi vs. EV transfected muscles at 7 days post. **(B & C)** RNAi transfected muscles displayed a significant reduction (~17%, *P* = 0.05) in muscle protein synthesis and **(D)** decreased phosphorylation levels of ERK1/2 (p44/42 MAPK) *(P* = 0.03). (E). p90RSK phosphorylation levels were significantly elevated (*P* = 0.04) in UBR5 RNAi transfected muscles verses the EV group. **(F)** Western blot images of puromycin (MPS) and phosphorylation of MAPK signalling targets *(n* = 5 per group – EV control and UBR5 RNAi). Data presented as Mean ± SEM.

Prolonged UBR5 RNAi transfection leads to significant loss of muscle mass and fibre CSA atrophy in mouse skeletal muscle

Given the data over 7 days, the next question to interrogate was the impact of UBR5 RNAi transfection in TA muscle for a prolonged period (30 days), with the hypothesis that this would lead to greater muscle atrophy vs. 7 days of UBR5 suppression. In line with the hypothesis, a significant reduction in muscle mass (-4.6 ± 1.5%) in UBR5 RNAi transfected vs. EV muscles was evident after 30 days (P = 0.01; Figure 7A). Alongside the reduction in muscle mass, a significant reduction in GFP-positive fibre CSA (-18.2 ± 2.3%) was evident after UBR5 RNAi transfection (*P* = 0.01; Figure 7B & C) vs. EV control, with the RNAi transfected muscles displaying a shift in the distribution of fibre CSA primarily towards smaller fibres (≥ 2600 µm^2) compared to the EV control muscle (Fig. 7B & 7D). These observations provide strong support towards the role of UBR5 as a positive modulator of muscle mass size.

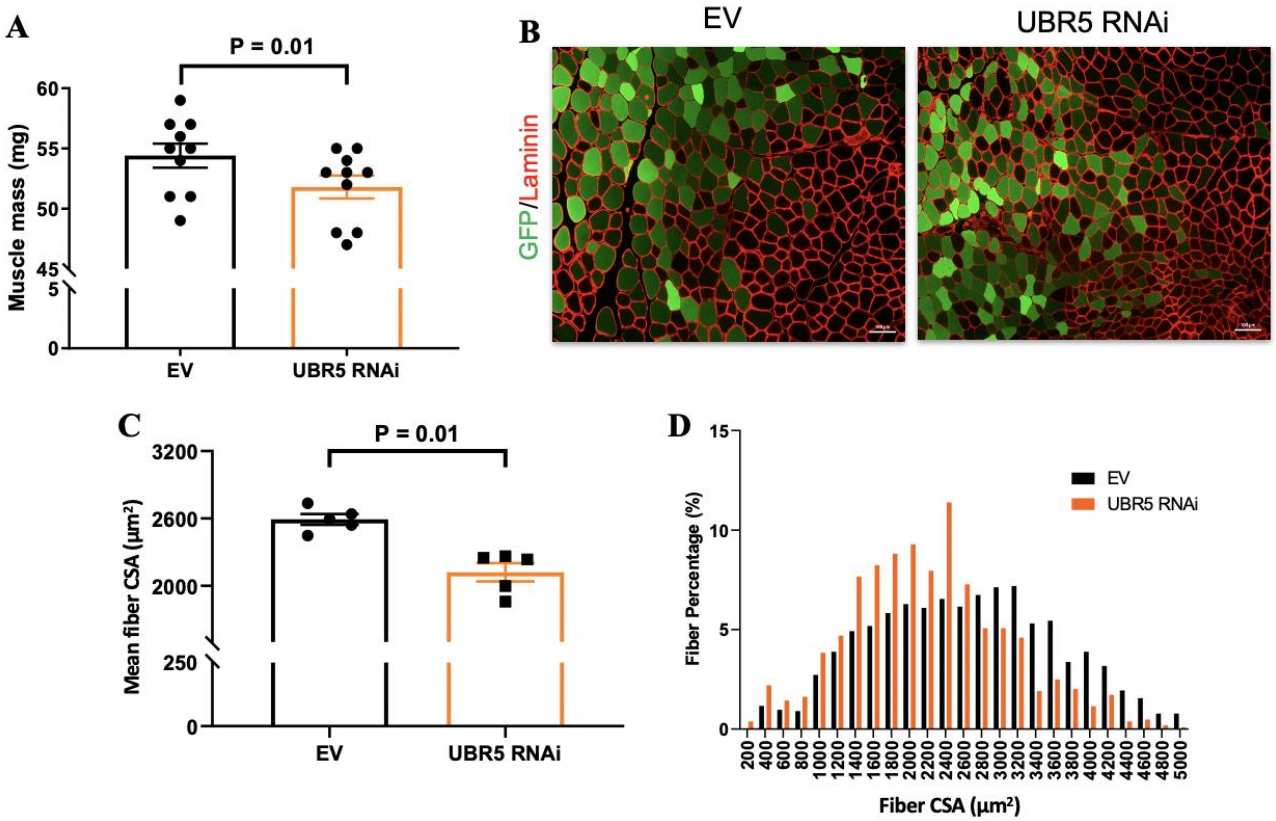

Figure 7. Loss of muscle mass and fibre CSA in UBR5 RNAi transfected TA muscle after 30 days. (**A)** After 30 days, muscle mass was significantly reduced in UBR5 RNAi transfected vs. empty vector control (EV) TA muscles (P = 0.01; *n* = 10 per group). **(B)** Representative images (10x magnification; scale bar = 100 µm) for GFP transfected fibre identification and CSA quantification through Laminin staining. **(C)** A significant reduction (*P* = 0.01) in mean transfected fibre CSA size was observed in the RNAi transfected vs. EV muscles *(n* = 5 per group). **(D)** Quantification of transfected muscle CSA revealed a leftward shift from large to smaller fibre sizes (≥3400 µm^2) with RNAi transfected muscles verses EV group (**D**). Data presented as Mean ± SEM.

Discussion

The present study aimed to: 1) silence UBR5 in human myotubes using siRNA during mechanical loading to confirm whether UBR5 was regulated in response to mechanical loading. Given MEK/ERK/p90RSK signalling has been associated with load-induced anabolism and hypertrophy, and altered with UBR5 manipulation in non-muscle cells, we also aimed to: 2) investigate the impact of reduced UBR5 on MEK/ERK/p90RSK signalling in SkM tissue using our miR-based RNAi for UBR5 electroporated into the tibialis anterior (TA) of mice. Mechanical loading of non-treated myotubes induced a non-significant increase in UBR5 gene expression which was similar to that following acute loading in murine bioengineered SkM (Seaborne *et al.*, 2019) and acute RE in humans (Seaborne *et al.*, 2018*a*, 2018*b*). Furthermore, mechanical loading was able to prevent the siRNA-induced reduction in UBR5 gene expression, which suggests that UBR5 gene expression may be activated downstream of mechano-sensitive signalling. Indeed, transfection of UBR5 RNAi into the

TA muscle of mice after 7 days caused a significant reduction in fibre CSA, total RNA, global protein synthesis and ERK1/2 phosphorylation. However, p90RSK phosphorylation significantly increased, suggestive of a potential compensatory mechanism triggered by the reduction in UBR5 and protein synthesis. The changes at 7 days also culminated in significant reductions in muscle mass and fibre CSA after prolonged (30 days) UBR5 RNAi. Overall, the present study further supports the notion that UBR5 plays an important role in muscle anabolism and hypertrophy.

The reduction in UBR5 gene expression is prevented by mechanical loading in myotubes

In the present study, transfection of UBR5 targeting siRNAs induced a ~77% reduction in UBR5 mRNA expression at 3 hrs in non-loaded human myotubes. Following confirmation of effective UBR5 knockdown in non-loaded myotubes, UBR5 gene expression was assessed in response to mechanical loading. Mechanical loading of non-treated myotubes displayed a non-significant increase (~1.58-fold) in UBR5 gene expression (see Figure 4B), which was similar to the fold changes observed (~1.71-fold) after an acute bout of RE in human SkM (Seaborne *et al.*, 2018*b*, 2018*a*) and acute loading in bioengineered SkM (~1.58-fold) (Seaborne *et al.*, 2019). Significant changes in UBR5 gene expression were achieved following chronic (7 weeks) training, and in retraining for which greatest increase in UBR5 gene expression was observed (Seaborne *et al.*, 2018*a*, 2018*b*). Also, UBR5 significantly increases after hypertrophy following 4 weeks of resistance training via programmed chronic high-frequency electrical stimulation in rats (Schmoll *et al.*, 2018; Seaborne *et al.*, 2019). Furthermore, we have previously reported a significant increase in UBR5 following acute loading in bioengineered C_2C_{12} SkM (Seaborne *et al.*, 2019). Despite a lack of significance, the acute stimulus and human variation may therefore explain the lack of statistical significance reported in UBR5 mRNA expression after loading in human myotubes in this study. However, the ~1.58-fold increases in UBR5 in human myotubes after mechanical loading in the present study reflects similar fold increases previously observed in mechanically loaded bioengineered C_2C_{12} SkM (~1.58-fold) and similar fold increases seen in human muscle after an acute bout of resistance exercise (~1.71-fold; Seaborne *et al.*, 2018*b*, 2018*a*, 2019).

The most striking finding reported in the human myotube data, is that mechanical loading was able to prevent the siRNA-induced reduction in UBR5 gene expression. Such findings suggest that UBR5 may act downstream of a mechano-sensitive pathway that is increased after loading. Indeed, the most relevant load-induced pathway in the context of UBR5 appears to be MEK/ERK/p90RSK signalling as this has been associated with altered UBR5 in non-muscle cells (Eblen *et al.*, 2003; Cho

et al., 2017). Where UBR5 has been shown to be a target substrate for ERK2 in COS-1 kidney fibroblast cell line cells after treatment with epidermal growth factor (Eblen *et al.*, 2003). It has also been reported that the ribosomal S6 kinase, p90RSK, phosphorylates UBR5 in HeLa cancer cells at numerous sites, and may be involved in cancer cell growth (Cho *et al.*, 2017). Given that ERK/p90RSK signalling is associated with human skeletal muscle growth (Drummond *et al.*, 2009) and load induced hypertrophy in rodents (Miyazaki *et al.*, 2011), assessing this MAPK signalling within the context of UBR5 RNAi in skeletal muscle tissue was a subsequent focus of our experiments.

Muscle fibre CSA, total RNA, protein synthesis, ERK1/2 signalling was reduced, but p90RSK signalling increased in UBR5 RNAi electroporated mouse muscle

Despite previous work by our group demonstrating increased UBR5 expression during SkM anabolism and hypertrophy (Seaborne *et al.*, 2018*b*, 2018*a*, 2019), no studies to date have reported the signalling responses associated with UBR5 manipulation in SkM. Given MEK/ERK/p90RSK signalling is pertinent for load-induced anabolism and hypertrophy in SkM (Hornberger *et al.*, 2005; Drummond *et al.*, 2009; Miyazaki *et al.*, 2011), and that this mechano-sensitive pathway is linked to UBR5 in non-muscle cells (Eblen *et al.*, 2003; Cho *et al.*, 2017), we next performed UBR5-specific knockdown experiments in mouse TA muscle (reduction of 55 and 60% UBR5 mRNA and protein levels, respectively), to investigate the impact of reduced UBR5 on MEK/ERK/p90RSK signalling *in-vivo*. Electroporation of UBR5 RNAi for 7 days induced a significant reduction in average myofibre CSA, frequency of larger myofibres (≥3400 μm^2), total RNA and muscle protein synthesis (~17%) which coincided with a reduction in ERK1/2 signalling (see Figures 5 & 6). The reduction in total RNA and muscle protein synthesis is interesting given the classification of UBR5 as an E3 ubiquitin ligase and thus its role in the ubiquitin-proteasome system. However, UBR5 has been suggested to have a role in the regulation of mRNA translation and gene regulation through the MLLE domain on the UBR5 protein structure (Xie *et al.*, 2014; Muńoz-Escobar *et al.*, 2015). Recent studies have identified the translation capacity and activity of skeletal muscle to be important for growth and hypertrophy in rodent and human models (Nakada *et al.*, 2016; Stec *et al.*, 2016; West *et al.*, 2016; Hammarström *et al.*, 2020). Our data potentially highlights the role of UBR5 in the regulation of translational capacity in SkM mass, a finding that warrants further investigation.

Interestingly, p90RSK signalling significantly increased following UBR5 knockdown which may be a consequence of the reduction in UBR5 and total protein synthesis observed in electroporated TA muscle, perhaps suggestive of a compensatory mechanism to control the level of reduced protein

synthesis and possibly subsequent muscle mass. Further, the increase in p90RSK signalling may occur due to its suggested role as an upstream regulator of UBR5 and its activation is altered due to the suppression of UBR5 protein levels (Cho *et al.*, 2017). This perhaps suggests that loss of UBR5 may mean that p90RSK is activated because its normal target for action is no longer present. In addition to acute alterations in ERK/p90RSK signalling and protein synthesis, prolonged transfection of the UBR5 RNAi for 30 days resulted in significant decreases in both muscle mass and fibre CSA. Taken together, the increase in UBR5 expression observed across various models of loading/RE in this present and in previous work by our group (Seaborne *et al.*, 2018*b*, 2018*a*, 2019), and the signalling responses reported herein, suggest reductions in UBR5 are associated with alterations in ERK/p90RSK signalling during SkM anabolism and hypertrophy.

Despite the exciting and novel findings surrounding UBR5's mechano-responses and associated signalling reported herein, it is worth acknowledging the limitations of the present study. Firstly, neither puromycin incorporation nor subsequent measures of total protein synthesis were assessed in human myotubes. This was due to the limited cellular material available during experimentation. It was therefore not feasible to extract protein for all conditions, nor to examine MAPK signalling in siUBR5 treated vs. non-treated human myotubes. Furthermore, hypertrophy experiments (e.g. synergistic ablation) were not performed in rodents, thus, we were unable to determine the MEK/ERK/p90RSK signalling responses in UBR5 RNAi vs. EV transfected TA muscle after hypertrophy. Taken together, future studies should wish to ascertain MEK/ERK/p90RSK activity in SkM with reduced UBR5 expression following hypertrophic stimuli.

Author contributions

DCT, DCH, SCB, APS conceived and designed the research. All authors were involved in acquisition or analysis or interpretation of data for the work. DCT, DCH, SCB, APS drafted the work. All Authors were involved in revising the work critically for important intellectual content. All authors approved the final version of the manuscript.

Funding

DCT was funded via PhD studentships from Keele University and Liverpool John Moores University (LJMU) via APS. DCTs project was further supported by the Society for Endocrinology equipment grant and the North Staffordshire Medical Institute awarded to APS. RAS was funded by Doctoral Alliance/ LJMU funded PhD studentship via APS and further supported by grants awarded to APS

from GlaxoSmithKline. PG was funded by EPSRC/MRC (UKRI) PhD studentship via APS and Keele University doctoral training centre and is now supported by the Norwegian School of Sport Sciences. DCH & LMB was supported by the University of Iowa in the laboratory of SCB.

Declarations & Competing Interests

SCB is on the scientific advisory board for Emmyon Inc. The authors declare that they have no other competing interests.

Data Availability Statement

The data that support the findings of this study are available from the corresponding author upon reasonable request.

Acknowledgments

We wish to thank Dr. David S. Waddell (University of North Florida) for technical assistance with the project.

References

Baar K, Torgan CE, Kraus WE & Esser K (2000). Autocrine Phosphorylation of p70 S6k in Response to Acute Stretch in Myotubes. *Mol Cell Biol Res Commun* **4,** 76–80.

Baehr LM, West DWD, Marcotte G, Marshall AG, De Sousa LG, Baar K & Bodine SC (2016). Age-related deficits in skeletal muscle recovery following disuse are associated with neuromuscular junction instability and ER stress, not impaired protein synthesis. *Aging (Albany NY)* **8,** 127–146.

Baehr LM, West DWD, Marshall AG, Marcotte GR, Baar K & Bodine SC (2017). Muscle-specific and age-related changes in protein synthesis and protein degradation in response to hindlimb unloading in rats. *J Appl Physiol* **122,** 1336–1350.

Bodine SC & Baehr LM (2014). Skeletal muscle atrophy and the E3 ubiquitin ligases MuRF1 and MAFbx/atrogin-1. *Am J Physiol - Endocrinol Metab* **307,** E469–E484.

Bodine SC, Latres E, Baumhueter S, Lai VKM, Nunez L, Clarke BA, Poueymirou WT, Panaro FJ,

Erqian Na, Dharmarajan K, Pan ZQ, Valenzuela DM, Dechiara TM, Stitt TN, Yancopoulos GD & Glass DJ (2001*a*). Identification of ubiquitin ligases required for skeletal Muscle Atrophy. *Science (80-)* **294,** 1704–1708.

Bodine SC, Stitt TN, Gonzalez M, Kline WO, Stover GL, Bauerlein R, Zlotchenko E, Scrimgeour A, Lawrence JC, Glass DJ & Yancopoulos GD (2001*b*). Akt/mTOR pathway is a crucial regulator of skeletal muscle hypertrophy and can prevent muscle atrophy in vivo. *Nat Cell Biol* **3,** 1014–1019.

Cao PR, Kim HJ & Lecker SH (2005). Ubiquitin-protein ligases in muscle wasting. *Int J Biochem Cell Biol* **37,** 2088–2097.

Cho JH, Kim SA, Seo YS, Park SG, Park BC, Kim JH & Kim S (2017). The p90 ribosomal S6 kinase–UBR5 pathway controls Toll-like receptor signaling via miRNA-induced translational inhibition of tumor necrosis factor receptor–associated factor 3. *J Biol Chem* **292,** 11804–11814.

Crown A, He X, Holly J, Lightman S & Stewart C (2000). Characterisation of the IGF system in a primary adult human skeletal muscle cell model, and comparison of the effects of insulin and IGF-I on protein metabolism. *J Endocrinol* **167,** 403–415.

Drummond MJ, Fry CS, Glynn EL, Dreyer HC, Dhanani S, Timmerman KL, Volpi E & Rasmussen BB (2009). Rapamycin administration in humans blocks the contraction-induced increase in skeletal muscle protein synthesis. *J Physiol* **587,** 1535–1546.

Ebert SM, Dyle MC, Kunkel SD, Bullard SA, Bongers KS, Fox DK, Dierdorff JM, Foster ED & Adams CM (2012). Stress-induced skeletal muscle Gadd45a expression reprograms myonuclei and causes muscle atrophy. *J Biol Chem* **287,** 27290–27301.

Eblen ST, Kumar NV, Shah K, Henderson MJ, Watts CKW, Shokat KM & Weber MJ (2003). Identification of novel ERK2 substrates through use of an engineered kinase and ATP analogs. *J Biol Chem* **278,** 14926–14935.

Goldberg A (1967). Work-induced growth of skeletal muscle in normal and hypophysectomized

rats. *Am J Physiol* **213,** 1193–1198.

Gomes MD, Lecker SH, Jagoe RT, Navon A & Goldberg AL (2001). Atrogin-1, A Muscle-Specific F-Box Protein Highly Expressed during Muscle Atrophy Author(s): *PNAS* **98,** 14440–14445.

Goodman CA, Frey JW, Mabrey DM, Jacobs BL, Lincoln HC, You JS & Hornberger TA (2011*a*). The role of skeletal muscle mTOR in the regulation of mechanical load-induced growth. *J Physiol* **589,** 5485–5501.

Goodman CA, Mabrey DM, Frey JW, Miu MH, Schmidt EK, Pierre P & Hornberger TA (2011*b*). Novel insights into the regulation of skeletal muscle protein synthesis as revealed by a new nonradioactive in vivo technique . *FASEB J* **25,** 1028–1039.

Hammarström D, Øfsteng S, Koll L, Hanestadhaugen M, Hollan I, Apró W, Whist JE, Blomstrand E, Rønnestad BR & Ellefsen S (2020). Benefits of higher resistance-training volume are related to ribosome biogenesis. *J Physiol* **598,** 543–565.

Heinemeier KM, Olesen JL, Haddad F, Schjerling P, Baldwin KM & Kjaer M (2009). Effect of unloading followed by reloading on expression of collagen and related growth factors in rat tendon and muscle. *J Appl Physiol* **106,** 178–186.

Hornberger TA, Armstrong DD, Koh TJ, Burkholder TJ & Esser KA (2005). Intracellular signaling specificity in response to uniaxial vs . multiaxial stretch : implications for mechanotransduction. *Am J Physiol Physiol* **288,** C185–C194.

Hughes DC, Marcotte GR, Baehr LM, West DWD, Marshall AG, Ebert SM, Davidyan A, Adams CM, Bodine SC & Baar K (2018). Alterations in the muscle force transfer apparatus in aged rats during unloading and reloading: impact of microRNA-31. *J Physiol* **596,** 2883–2900.

Hunt LC, Stover J, Haugen B, Shaw TI, Li Y, Pagala VR, Finkelstein D, Barton ER, Fan Y, Labelle M, Peng J & Demontis F (2019). A Key Role for the Ubiquitin Ligase UBR4 in Myofiber Hypertrophy in Drosophila and Mice. *Cell Rep* **28,** 1268–1281.

Miyazaki M, Mccarthy JJ, Fedele MJ & Esser KA (2011). Early activation of mTORC1 signalling in

response to mechanical overload is independent of phosphoinositide 3-kinase/Akt signalling. *J Physiol* **589,** 1831–1846.

Moore DR, Atherton PJ, Rennie MJ, Tarnopolsky MA & Phillips SM (2011). Resistance exercise enhances mTOR and MAPK signalling in human muscle over that seen at rest after bolus protein ingestion. *Acta Physiol* **201,** 365–372.

Muńoz-Escobar J, Matta-Camacho E, Kozlov G & Gehring K (2015). The MLLE domain of the ubiquitin ligase UBR5 binds to its catalytic domain to regulate substrate binding. *J Biol Chem* **290,** 22841–22850.

Nakada S, Ogasawara R, Kawada S, Maekawa T & Ishii N (2016). Correlation between ribosome biogenesis and the magnitude of hypertrophy in overloaded skeletal muscle. *PLoS One* **11,** 1–14.

Owens DJ, Sharples AP, Polydorou I, Alwan N, Donovan T, Tang J, Fraser WD, Cooper RG, Morton JP, Stewart C & Close GL (2015). A systems-based investigation into vitamin D and skeletal muscle repair, regeneration, and hypertrophy. *Am J Physiol - Endocrinol Metab* **309,** E1019–E1031.

Schmittgen TD & Livak KJ (2008). Analyzing real-time PCR data by the comparative CT method. *Nat Protoc* **3,** 1101–1108.

Schmoll M, Unger E, Sutherland H, Haller M, Bijak M, Lanmuller H & Jarvis JC (2018). SpillOver stimulation : A novel hypertrophy model using co-contraction of the plantar- flexors to load the tibial anterior muscle in rats. *PLoS One* **13,** 1–19.

Seaborne R., Hughes DC, Turner DC, Owens DJ, Baehr LM, Gorski P, Semenova EA, Borisov O V., Larin AK, Popov D V., Generozov E V., Sutherland H, Ahmetov II, Jarvis JC, Bodine SC & Sharples AP (2019). UBR5 is a novel E3 ubiquitin ligase involved in skeletal muscle hypertrophy and recovery from atrophy. *J Physiol* **597,** 3727–3749.

Seaborne R., Strauss J, Cocks M, Shepherd S, O'Brien T., van Someren K., Bell P., Murgatroyd C,

Morton J., Stewart C., Mein C. & Sharples A. (2018*a*). Data Descriptor : Methylome of human skeletal muscle after acute & chronic resistance exercise training , detraining & retraining. *Sci Data* **5,** 1–9.

Seaborne R., Strauss J, Cocks M, Shepherd S, O'Brien T., Van Someren K., Bell P., Murgatroyd C, Morton J., Stewart C. & Sharples A. (2018*b*). Human Skeletal Muscle Possesses an Epigenetic Memory of Hypertrophy. *Sci Rep* **8,** 1–17.

Stec MJ, Kelly NA, Many GM, Windham ST, Tuggle SC & Bamman MM (2016). Ribosome biogenesis may augment resistance training-induced myofiber hypertrophy and is required for myotube growth in vitro. *Am J Physiol - Endocrinol Metab* **310,** E652–E661.

Turner DC, Kasper AM, Seaborne RA, Brown AD, Close GL, Murphy M, Stewart CE, Martin NRW & Sharples AP (2019*a*). Exercising Bioengineered Skeletal Muscle In Vitro: Biopsy to Bioreactor. In *Methods in Molecular Biology*, Myogenesis., ed. Rønning S., pp. 55–79. Springer International Publishing, New York, NY.

Turner DC, Seaborne RA & Sharples AP (2019*b*). Comparative Transcriptome and Methylome Analysis in Human Skeletal Muscle Anabolism , Hypertrophy and Epigenetic Memory. *Sci Rep* **9,** 1–12.

Wen Y, Murach KA, Vechetti IJ, Fry CS, Vickery C, Peterson CA, McCarthy JJ & Campbell KS (2018). Myo Vision: Software for automated high-content analysis of skeletal muscle immunohistochemistry. *J Appl Physiol* **124,** 40–51.

West DWD, Baehr LM, Marcotte GR, Chason CM, Tolento L, Gomes A V., Bodine SC & Baar K (2016). Acute resistance exercise activates rapamycin-sensitive and -insensitive mechanisms that control translational activity and capacity in skeletal muscle. *J Physiol* **594,** 453–468.

Williamson D, Gallagher P, Harber M, Hollon C & Trappe S (2003). Mitogen-activated protein kinase (MAPK) pathway activation: Effects of age and acute exercise on human skeletal muscle. *J Physiol* **547,** 977–987.

Xie J, Kozlov G & Gehring K (2014). The “tale” of poly(A) binding protein: The MLLE domain and PAM2-containing proteins. *Biochim Biophys Acta - Gene Regul Mech* **1839,** 1062–1068.

Yu M, Blomstrand E, Chibalin A V., Krook A & Zierath JR (2001). Marathon running increases ERK1/2 and p38 MAP kinase signalling to downstream targets in human skeletal muscle. *J Physiol* **536,** 273–282.

First Author Profiles

Daniel Turner completed his BSc and MSc degrees in Exercise Science and Nutrition at Liverpool John Moores University (LJMU) from 2012-2016. He then completed his PhD in Cellular and Molecular Exercise Physiology at LJMU/Keele University (2016-2020) which entailed using a bioengineered skeletal muscle model to study the transcriptional and epigenetic response to loading *in-vitro*. During his PhD, Daniel also conducted epigenetic analysis in aged human muscle tissue and cells derived from orthopaedic patients. His future research wishes to continue addressing the molecular responses to loading/unloading and nutrition using both *in-vitro* and *in-vivo* skeletal muscle models.

David Hughes completed his Bachelor and Masters degrees in Exercise Science at Manchester Metropolitan University (2005-2009). He then went on to complete his PhD in Muscle Cell Physiology at the University of Bedfordshire/ Liverpool John Moores University (2010-2014). For the past 6 years he has undertaken postdoctoral research training in the USA. His research has focused on cytoskeleton proteins in aging skeletal muscle and more recently, novel E3 ubiquitin ligases in muscle atrophy/remodeling. To date his work has utilized in vitro and in vivo models to target novel areas of muscle physiology and probe important questions that remain in aging and disease.